Radial Basis Function Neural Network-Based Super-Twisting Blade Pitch Controller for the Floating Offshore Wind Turbine

Flavie Didier[1], Yong-Chao Liu[1] and Salah Laghrouche[1]

***Abstract*— The study introduces a novel Radial Basis Function Neural Network-based Super-Twisting Sliding Mode Collective Blade Pitch Control (RBFNN-STSM-CBPC), designed specifically for semi-submersible platform-based Floating Offshore Wind Turbines (FOWTs) operating above rated speed (Region III). The proposed composite controller is developed using a refined nonlinear Control-Oriented Model, including lumped unmodeled dynamics and external disturbances. To our knowledge, this is the first time that a neural network STSM-CPBC approach is designed for this application. The RBFNN operates as an adaptive observer for the lumped disturbance, enhancing the robustness and performance of the standard STSM-CBPC for the same gains. Its adaptive law, formulated through the Lyapunov method, ensures stability and convergence by adjusting the adaptive weight. Simulation results demonstrate the superiority of the RBFNN-STSM-CBPC over the standard STSM-CBPC method in regulating rotor speed and mitigating platform motion.**

I. INTRODUCTION

The global commitment to reduce CO_2 emissions and lower fossil fuel consumption, coupled with the increasing energy demand, is driving rapid advancements in renewable energy technologies. Departing from traditional bottom-fixed installations, Floating Offshore Wind Turbines represent a significant innovation in the field of wind energy. The floating platform allows the deployment of wind turbines farther from the coast, enabling large-scale implementation with reduced visibility. Moreover, FOWT systems harness superior wind resources in terms of increased intensity and reduced turbulence, thereby enhancing power extraction. The wind turbine's operating range is divided into four regions based on incoming wind speed, each with specific control objectives. In operating Region III, where the wind speeds surpass the rated speed, the primary control objective is to regulate generated power at its rated value. However, the development of adaptive and robust controllers becomes challenging due to the nonlinear dynamics inherent in FOWT systems. The floating nature of FOWTs introduces additional dynamics, including hydrodynamic and mooring dynamics, as well as combined environmental loads such as wind, waves, and currents, leading to a complex nonlinear system. Especially in Region III, the apparition of the negative damping phenomenon [1] can induce instability in the platform pitching motion. Therefore, controllers must not only ensure rated power extraction but also minimize structural movements. This paper addresses these challenges with a focus on developing a model-based collective blade pitch control to ensure optimal performance.

Conventional control methods derived from fixed wind turbines have been adapted to FOWT systems. A Gain Scheduling Proportional Integral (GSPI) controller was employed in [2] to mitigate the negative damping phenomenon by adjusting the rotor speed based on the blade angle activity. This configuration is commonly regarded as the baseline controller for FOWTs, serving as a benchmark for testing newly developed controllers. However, these adapted conventional controllers remain sensitive to external disturbances and lack robustness against unmodelled dynamics. Several linear controllers have been proposed, leveraging simplify nonlinear models [3], [4], [5] of system dynamics. These simplified models are linearized around an operating point for the implementation of linear control systems, leading to performance degradation when the turbine operates away from the defined operating point.

Nonlinear controllers, particularly Sliding Mode Controllers (SMCs), have proven effective in managing external disturbances and model uncertainties for a large range of nonlinear systems. Employing discontinuous control signals, SMC guarantees the convergence of the sliding variable to the origin in finite time, with gains determined using upper-bound information regarding disturbances and uncertainties. However, the inherent discontinuity in the control input can result in chattering effects, leading to over-actuation and performance degradation. Addressing these challenges, the Super-Twisting algorithm-based Sliding Mode (STSM) controller has been employed for its high-performance characteristics. Considering Region III control challenges for FOWT systems, researchers have developed a first-order SMC based on a reduced model in [6]. Additionally, an STSM controller has been effectively implemented in [7] and [8], leveraging a linear model generated by OpenFAST [9]. Adopting a continuous approach with adaptive methods, an adaptive form of the STSM controller has been employed in [10], showcasing superior performance in terms of rotor speed control, power regulation, and reduction of the platform pitch motion when compared to traditional GSPI approaches. Furthermore, in [11], a new iteration of the adaptive STSM controller has been designed, featuring adaptive laws with two parameters and applied to the FOWT system in Region III.

Nevertheless, the STSM controller's use of the bounded sign function results in slower convergence of the sliding variable when far away from the origin [12]. To enhance convergence, gains must be increased, exacerbating chattering

[1]The authors are with FEMTO-ST Institutes (UMR 6174), Université Franche-Comté, UTBM, CNRS, Belfort, France flavie.didier@utbm.fr

effects. To overcome this limitation, an artificial neural network can be employed as a model-free disturbance observer to assist the STSM control in dealing with uncertainties and disturbance within the model. As neural networks exhibit significant capabilities in approximating a wide range of nonlinear functions, when integrated with STSM controller, they enhance the system's robustness. The resulting composite controller design achieve control objectives and disturbance attenuation through the controller-based feedback regulation mechanism and the neural network estimator, respectively. The Radial Basis Function Neural Network (RBFNN) represents a well-explored class of neural network known for its simple and widely investigated network structure. Previous research has explored the application of RBFNN in combination with SMC for nonlinear systems. For instance, [13] presents a robust adaptive SMC strategy based on an RBFNN for time-varying systems. In [14], a SMC scheme based on an RBFNN is proposed for robotic manipulators, where the RBF network approximates the nonlinear dynamics of the robot. Additionally, RBFNN-based STSM controller has also been studied for MEMS gyroscopes [15].

This paper introduces the design of an innovative RBFNN-based STSM Collective Blade Pitch Controller (RBFNN-STSM-CBPC) for the semi-submersible FOWT [16]. Leveraging the rearranged Homer nonlinear Control-Oriented Model (COM) [17], the RBFNN-STSM-CBPC aims to regulate rotor speed at its rated value while minimizing platform pitch motion in Region III. Given the intricate nature of FOWT modeling, the RBFNN is employed to effectively capture unknown model uncertainties and disturbances, facilitating controller design based on the nonlinear COM without necessitating an exact mathematical model. This novel composite controller combines a STSM controller with a RBFNN disturbance observer, and an error estimator to offset the theoretical minimum estimation error inherent in the RBFNN, thereby enhancing system robustness and improving control performance.

The paper is organized as follows: In Section II, the Homer nonlinear COM is presented, along with the reformulation of the necessary dynamics for developing the model-based controller in Region III. Section IV presents the design of the RBFNN-STSM-CBPC along with the control objectives. Section V validates the proposed CBPC through comparative co-simulation test. Finally, Section VI concludes the paper.

II. FOWT System Modelling

The specific semi-submersible FOWT considered in this study is the NREL OC4-DeepCwind 5 MW semi-submersible FOWT [16]. In the derivation of the control laws, the Homer nonlinear COM [5] has been chosen, serving as the foundation for designing nonlinear controllers. This section provides a partial presentation of the selected model, outlining the necessary dynamic reformulations required to facilitate the design of effective nonlinear controllers.

A. Considered COM

The considered semi-submersible FOWT, composed of the floating platform and wind turbine is regarded as a single rigid body. In this study, the nacelle yaw motion is neglected and the one-mass rigid shaft model expressed as (1) is selected as the dynamic model of the drive-train:

$$\dot{\omega_r} = \frac{1}{J_l}(\frac{P_A}{\omega_r} - n_g T_g) \tag{1}$$

where P_A is the aerodynamic power, n_g is the gearbox ratio, T_g is the generator torque, and J_l is the low-speed shaft equivalent inertia.

The states include x_m, y_m, z_m, θ_x, θ_y, θ_z and their time derivatives, as defined in [5]. Taking into account the adopted dynamic model of the drive-train, the other considered states are the rotor azimuth angle θ_r and the rotor speed ω_r. Thus, the state vector defined in this study is expressed as:

$$\mathbf{x} = [\mathbf{x}_m, \theta, \theta_r, \dot{\mathbf{x}}_m, \dot{\theta}, \omega_r]^\top \tag{2}$$

$$with \quad \mathbf{x}_m = [x_m, y_m, z_m] \quad and \quad \theta = [\theta_x, \theta_y, \theta_z].$$

The control input vector u includes the blade pitch angle β and the generator torque T_g.

$$u = [\beta, T_g]^\top \tag{3}$$

Based on [5], and considering the one-mass rigid shaft model (1), the equations of motion of the semi-submersible FOWT can be expressed as:

$$\begin{bmatrix} \ddot{\mathbf{x}}_m \\ \ddot{\theta} \\ \dot{\omega}_r \end{bmatrix} = \begin{bmatrix} (m_g \mathbf{I}_3 + m_a)^{-1} (\mathbf{F}_A + \mathbf{F}_B + \mathbf{F}_C + \mathbf{F}_D) \\ \mathbf{R}(\theta) \mathbf{I}_\theta^{-1} \mathbf{R}(\theta)^\top (\mathbf{T}_A + \mathbf{T}_B + \mathbf{T}_C + \mathbf{T}_D) \\ \frac{1}{J_l} \left(\frac{P_A}{\omega_r} - n_g T_g \right) \end{bmatrix} \tag{4}$$

$$= \mathbf{f}(\mathbf{x}, \mathbf{u}, \mathbf{v}, \mathbf{w})$$

$$with \quad \mathbf{R}(\theta) = \begin{bmatrix} 1 & -\theta_z & \theta_y \\ \theta_z & 1 & -\theta_x \\ -\theta_y & \theta_x & 1 \end{bmatrix} \tag{5}$$

where m_g is the total mass of the FOWT, m_a is the hydrodynamic added mass vector, $\mathbf{F}_A$, $\mathbf{F}_B$, $\mathbf{F}_C$, $\mathbf{F}_D$ are the aerodynamic force vector, the buoyancy force vector, the mooring line force vector, the hydrodynamic drag and inertial force vector, respectively, $\mathbf{T}_A$, $\mathbf{T}_B$, $\mathbf{T}_C$, $\mathbf{T}_D$ are the aerodynamic torque vector, the buoyancy torque vector, the mooring line torque vector, the hydrodynamic drag and inertial torque vector, respectively, $\mathbf{I}_\theta$ is the inertia tensor of the FOWT, $\mathbf{R}(\theta)$ is the simplified rotation matrix, and $\mathbf{f} = (\mathbf{x}, \mathbf{u}, \mathbf{v}, \mathbf{w})$ is the nonlinear function vector describing the equations of motion, where $\mathbf{v}$ and $\mathbf{w}$ are the wind and wave disturbance vectors, respectively.

B. Model Reformulation for Nonlinear Model-Based Control

Given the high coupling between the states and control inputs in (4), direct design of the nonlinear controller using the dynamics of ω_r and $\dot{\theta}_y$ becomes challenging. Therefore, it is necessary to reformulate the dynamics of $\dot{\theta}_y$ and ω_r presented in (4).

In this study, a single thrust force F_A is used to represent all forces resulting from the interaction between the wind and the FOWT. This force acts at the center of thrust in the hub. Thus, F_A can be expressed as:

$$F_A = \frac{1}{2}\rho_a \pi R_r^2 C_t(\lambda, \beta) \left\|\mathbf{v}_n\right\|_2 \mathbf{v}_n \tag{6}$$

where ρ_a is the air density, R_r is the effective rotor radius, $\mathbf{v}_n$ is the equivalent velocity vector normal to the face of the rotor, C_t is the thrust coefficient that is a highly nonlinear function in terms of the tip speed ratio $\lambda = \frac{R_r \omega_r}{\|\mathbf{v}_n\|_2}$ and β, $\|\cdot\|_2$ denotes the Euclidean norm of a vector. Furthermore, the aerodynamic power P_A can be expressed as:

$$P_A = \frac{1}{2}\rho_a \pi R_r^2 C_p(\lambda, \beta) \left\|\mathbf{v}_n\right\|_2^3 \tag{7}$$

where C_p is the power coefficient, a highly nonlinear function in terms of λ and β.

Both thrust and power coefficients, $C_t(\lambda, \beta)$ and $C_p(\lambda, \beta)$ are modeled by polynomial functions and rearranged as:

$$\begin{aligned} C_t(\lambda, \beta) &= g_{ct}\beta + f_{ct} \\ C_p(\lambda, \beta) &= g_{cp}\beta + f_{cp} \end{aligned} \tag{8}$$

where g_{ct}, g_{cp}, f_{ct} and f_{cp} are polynomial functions of λ.

Based on (4), substituting (8) into (6)-(7), and taking the external disturbances, parametric uncertainties and unmodeled dynamics into account, the dynamics of $\dot{\theta_y}$ and ω_r can be rewritten as:

$$\begin{aligned} \dot{\omega}_y = \ddot{\theta}_y &= g_y\beta + H_y \\ \dot{\omega}_r = \ddot{\theta}_r &= g_r\beta + H_r \end{aligned} \tag{9}$$

where ω_y is the platform pitch rate, g_y and g_r are nonlinear function of ω_y and ω_r respectively, H_y and H_r are considered lumped uncertainties and external disturbances, defined as:

$$\begin{cases} g_y = d_\theta g_{ct} \left\|v_n\right\|_2^2 (\theta_x^2 + \theta_y^2 + \theta_z^2 + 1) \\ H_y = d_\theta f_{ct} \left\|v_n\right\|_2^2 (\theta_x^2 + \theta_y^2 + \theta_z^2 + 1) + D_{\theta_y} \end{cases} \tag{10}$$

$$\begin{cases} g_r = \frac{\rho_a \pi R_r^2}{2 J_l \omega_r} g_{cp} \left\|v_n\right\|_2^3 \\ H_r = \frac{\rho_a \pi R_r^2}{2 J_l \omega_r} f_{cp} \left\|v_n\right\|_2^3 - \frac{n_g}{J_l} T_g \end{cases} \tag{11}$$

with D_{θ_y} and d_θ expressed as in [18].

Assumption 1: H_y and its time derivative $\dot{H}_y$ are bounded such that $|H_y| \leq \rho_{y1}$ and $|\dot{H}_y| \leq \rho_{y2}$ for two positive constants ρ_{y1} and ρ_{y2}.

Assumption 2: H_r and its time derivative $\dot{H}_r$ are bounded such that $|H_r| \leq \rho_{r1}$ and $|\dot{H}_r| \leq \rho_{r2}$ for two positive constants ρ_{r1} and ρ_{r2}.

III. Control Design

This section presents the design of the RBFNN-STSM-CBPC for the FOWT system in Region III. This CBPC consists of three components: the standard STSM-CBPC, the RBFNN, and the error estimator.

A. Problem formulation

In Region III, the primary control objectives are the regulation of the generator power to its rated value, while ensuring stability in the platform pitching motion. The generator power P_g can be described by the following expression [19], [16]:

$$P_g = \eta_e \eta_g T_g \omega_r \tag{12}$$

where η_e is the generator efficiency.

Given that T_g is fixed at its rated value, the first control objective of regulating generator power is equivalent to maintaining the rotor speed at its rated value $\omega_{rd} = 12.1 rpm$, expressed as e_r. The second control objective, aiming at reducing platform pitching motion, is equivalent to driving the platform pitch rate ω_y to zero, expressed as e_y:

$$\begin{aligned} e_r &= \omega_r - \omega_{rd} \\ e_y &= \omega_y - 0 = \omega_y. \end{aligned} \tag{13}$$

The same control input β is found in both dynamics, resulting in an under-actuated control problem. To address this, the rated rotor speed ω_{rd} is modified from a fixed value to a linear function ω_{rd}^* correlated with the platform pitch rate:

$$\omega_{rd}^* = \omega_{rd}(1 - k_y \omega_y) \tag{14}$$

where k_y is a positive constant.

Hence, the control objective for the FOWT in Region III is to force the composite tracking error e expressed as (14) to zero:

$$\begin{aligned} e = \omega_r - \omega_{rd}^* &= \omega_r - \omega_{rd}(1 - k_y \omega_y) \\ &= e_r + k_s e_y \end{aligned} \tag{15}$$

where $k_s = k_y \omega_{rd}$ is a positive constant scalar with units of $rpm \cdot s/deg$.

B. Standard STSM-CBPC Design

Acknowledge for its robustness in handling uncertainties and disturbances, SMC stands as an effective choice for controlling nonlinear systems, while the super-twisting algorithm play a crucial role in alleviating chattering phenomena.

Based on (15) the proposed sliding variable is chosen as:

$$s = e_r + k_s e_y. \tag{16}$$

The first time derivative of s can be written as:

$$\dot{s} = \dot{e_r} + k_s \dot{e_y} = \dot{\omega_r} + k_s \dot{\omega_y}. \tag{17}$$

Substituting (9) into (17), the derivative can be expressed as:

$$\dot{s} = (g_r\beta + H_r) + k_s(g_y\beta + H_y) = g_s\beta + H_s \tag{18}$$

where $g_s = g_r + k_s g_y$ and $H_s = H_r + k_s H_y$ is the lumped uncertainties and external disturbance.

According to Assumption 1 and Assumption 2, $|H_s| \leq \rho_{s1}$ and $|\dot{H}_s| \leq \rho_{s2}$ hold for two positive constants $\rho_{s1} = \rho_{r1} + k_s \rho_{y1}$ and $\rho_{s2} = \rho_{r2} + k_s \rho_{y2}$.

The control law of the standard STSM control is then designed as:

$$\beta_{STSM} = \frac{1}{g_s}(-k_1\sqrt{|s|}sgn(s) - k_2\int sgn(s)d\tau) \quad (19)$$

where $k_1 > 0$ and $k_2 > 0$ are controller gains, and $sgn(\cdot)$ is the signum function.

To enhance the robustness and control performance of the presented standard STSM-CBPC controller, an RBFNN is integrated to attenuate disturbances.

C. RBFNN Design

The utilization of data-driven techniques, particularly artificial intelligence, for developing adaptive controllers for FOWTs has experienced significant growth [20]. Additionally, the integration of SMC with a RBFNN to create a composite controller has been a subject of research for an extended period. The RBFNN is specifically employed for estimating and compensating the lumped disturbance H_s in (18). The stability analysis is conducted to derive the adaptive laws for the weights of the adopted neural network. This section provides insight into the RBFNN structure and details the design of the RBFNN-STSM-CBPC.

The standard structure of an RBFNN consists of three layers: an input layer, a hidden layer, and an output layer as illustrated in Fig.1.

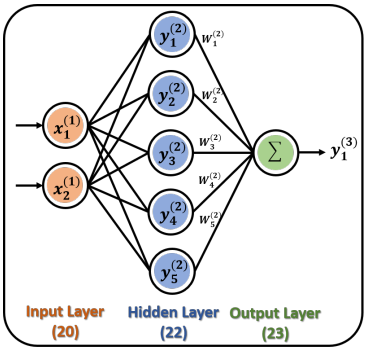

Fig. 1. RBFNN structure with a dimensionality of 25.

In this study, the signal propagation of the neural network is described as follows.

Input Layer: s and its time derivative $\dot{s}$ are selected as two input signals. As for output signals of the input layer, they are expressed as:

$$\begin{aligned} y_1^{(1)} &= x_1^{(1)} = s \\ y_2^{(1)} &= x_2^{(1)} = \dot{s} \end{aligned} \quad (20)$$

where $x_1^{(1)}$ and $x_2^{(1)}$ denote the input signals, while $y_1^{(1)}$ and $y_2^{(1)}$ represent the output signals of the input layer.

Hidden Layer: This layer employs N neurons. The signal propagation in the jth neuron is given as follows:

$$x_j^{(2)} = \frac{\left[y_1^{(1)} - c_{j1}\right]^2}{2\delta_{j1}^2} + \frac{\left[y_2^{(1)} - c_{j2}\right]^2}{2\delta_{j2}^2}, \quad (21)$$

$$y_j^{(2)} = e^{-x_j^{(2)}}, \quad with \quad j = 1, 2, \ldots, N \quad (22)$$

where $x_j^{(2)}$ and $y_j^{(2)}$ are the input and output signals, c_{j1} and c_{j2} are the centers, while δ_{j1} and δ_{j2} are the widths of two Gaussian functions, respectively.

Output Layer: The output signal denoted as $\hat{H}_s$, represents the estimated lumped disturbance in the s-dynamics and is expressed as follows:

$$\hat{H}_s = y_1^{(3)} = \mathbf{W}^{(2)\top}\mathbf{y}^{(2)} \quad (23)$$

where $\mathbf{W}^{(2)\top}$ and $\mathbf{y}^{(2)}$ are the hidden layer weight vector and output vector, respectively, and $y_1^{(3)}$ is the output signal.

Given the universal approximation property, there exists an optimal output weight vector $\mathbf{W}^{(2)}$ for the RBFNN enabling the expression of the lumped disturbance H_s as:

$$H_s = \mathbf{W}^{(2)*\top}(n)y^{(2)} + \varepsilon^* \quad (24)$$

where $\mathbf{W}^{(2)*\top}$ is the optimal hidden layer weight vector, ε^* is the minimum estimation error of the neural network. In this study, the value of $\mathbf{W}^{(2)}$ is updated online by derived learning laws.

D. RBFNN-STSM-CBPC Design

The design of the RBFNN-STSM-CBPC is presented in this subsection. The block diagram of the control system is represented in Fig.2.

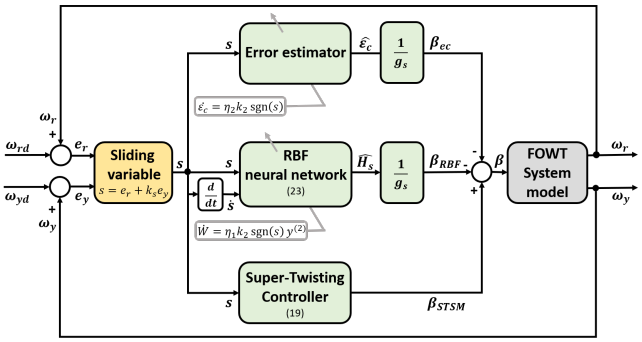

Fig. 2. Bloc diagram of the RBFNN-STSM-CBPC

The neural network aims to capture and estimate the unknown lumped disturbance denoted H_s. The input to the RBFNN is $\mathbf{x} = [s, \dot{s}]$, and the output of the RBFNN is, $\hat{H}_s$, expressed as (23), where the weight vector $\mathbf{W}^{(2)\top}$ is updated by an adaptive law derived from Lyapunov stability theory.

Then, considering the sliding variable s (16) and its dynamics $\dot{s}$ (17), the control law for the RBFNN-STSM-CBPC is formulated as follows:

$$\beta = \beta_{\text{STSM}} + \beta_{\text{RBF}} + \beta_{\text{ec}} \quad (25)$$

where β_{STSM} is the standard STSM-CBPC expressed as (19), β_{RBF} and β_{ec} are the RBFNN and the error estimators expressed as:

$$\beta_{\text{RBF}} = -\frac{1}{g_s}\hat{H}_s, \quad \beta_{\text{ec}} = -\frac{1}{g_s}\varepsilon_{ec} \quad (26)$$

where ε_{ec} is the term updated by the adaptive law online.

Substituting (25) into (18), the s-dynamics can be described as:

$$\begin{aligned}\dot{s} &= g_s\beta + H_s = -k_1\sqrt{|s|}sgn(s) - k_2\int sgn(s)d\tau \\ &\quad - \hat{H}_s - \varepsilon_{ec} + H_s \\ &= -k_1\sqrt{|s|}sgn(s) - k_2\int sgn(s)d\tau - \Delta\mathbf{W}^{(2)\top}\mathbf{y}^{(2)} - \Delta\varepsilon\end{aligned} \tag{27}$$

where $\Delta W^{(2)} = \mathbf{W}^{(2)} - \mathbf{W}^{(2)*}$ and $\Delta\varepsilon = \varepsilon_{ec} - \varepsilon^*$.

Assumption 3: $\mathbf{W}^{(2)*}$ and ε^* are considered to be constant in the derivation of the learning laws.

The following theorem establishes the criteria for selecting the control gains and learning laws of the RBFNN-STSM-CBPC to ensure the asymptotic convergence of s to the origin.

Theorem 1: Regarding the system (27), considering $k_1 > 0$ and $k_2 > 0$, if the learning laws are selected as (28), s will converge to the origin asymptotically.

$$\dot{\mathbf{W}}^{(2)\top} = \eta_1 k_2 \text{sgn}(s)\mathbf{y}^{(2)}, \quad \dot{\varepsilon}_{ec} = \eta_2 k_2 \text{sgn}(s) \tag{28}$$

where η_1 and η_2 denote positive learning rates. Proof: Firstly, the system (27) is converted to the following form.

$$\begin{cases}\dot{s} = -k_1\sqrt{|s|}\text{sgn}(s) - \Delta\mathbf{W}^{(2)T}\mathbf{y}^{(2)} - \Delta\varepsilon + \phi \\ \dot{\phi} = -k_2\text{sgn}(s)\end{cases} \tag{29}$$

Then, the following Lyapunov candidate function [21] is chosen for the system (29).

$$V = k_2|s| + \frac{1}{2}\phi^2 + \frac{1}{2\eta_1}\Delta\mathbf{W}^{(2)\top}\Delta\mathbf{W}^{(2)} + \frac{1}{2\eta_2}\Delta\varepsilon^2 \tag{30}$$

Based on Assumption 3 and (28), the first-time derivative of V is:

$$\begin{aligned}\dot{V} &= k_2\dot{s}sgn(s) + \phi\dot{\phi} + \frac{1}{\eta_1}\Delta\mathbf{W}^{(2)\top}\Delta\dot{\mathbf{W}}^{(2)} + \frac{1}{\eta_2}\Delta\varepsilon\Delta\dot{\varepsilon} \\ &= k_2(-k_1\sqrt{|s|}sgn(s) - \Delta\mathbf{W}^{(2)\top}\mathbf{y}^{(2)} - \Delta\varepsilon + \phi)sgn(s) \\ &\quad - \phi k_2 sgn(s) + \frac{1}{\eta_1}\Delta\mathbf{W}^{(2)\top}\Delta\dot{\mathbf{W}}^{(2)} + \frac{1}{\eta_2}\Delta\varepsilon\Delta\dot{\varepsilon} \\ &= -k_1k_2\sqrt{|s|} - \frac{1}{\eta_1}\Delta\mathbf{W}^{(2)\top}(\eta_1 k_2\mathbf{y}^{(2)}sgn(s) - \Delta\dot{\mathbf{W}}^{(2)}) \\ &\quad - \frac{1}{\eta_2}\Delta\varepsilon(\eta_2 k_2 sgn(s) - \Delta\dot{\varepsilon}) = -k_1k_2\sqrt{|s|}.\end{aligned} \tag{31}$$

Since $\dot{V} \leq 0$, $\dot{V}$ is negative semi-definite. Hence the asymptotic convergence of s to the origin can be demonstrated. The proof is completed.

IV. SIMULATIONS STUDY

To validate the effectiveness of the proposed CBPC, a comparative co-simulation test was conducted using Matlab/Simulink and OpenFAST. In this test, the performance of the proposed CBPC are compared with the standard STSM-CBPC (19) keeping the same values for k_1 and k_2, and the baseline controller [2].

TABLE I

RELATED PARAMETERS OF THE CONTROL SYSTEM

Parameter	Value	Parameter	Value
k_1	2	g_s	-2.6296
k_2	2	ω_{rd}	12.1
k_y	0.05	ω_{yd}	0

A. Simulations Conditions

OpenFAST is employed for simulating the NREL OC4-DeepCwind 5 MW semi-submersible FOWT. The wind and wave profiles in Fig.3 are characterized by a mean wind speed of 18 m/s with 15% turbulence, a wave height of 5.18 meters and a peak wave period of 12 seconds.

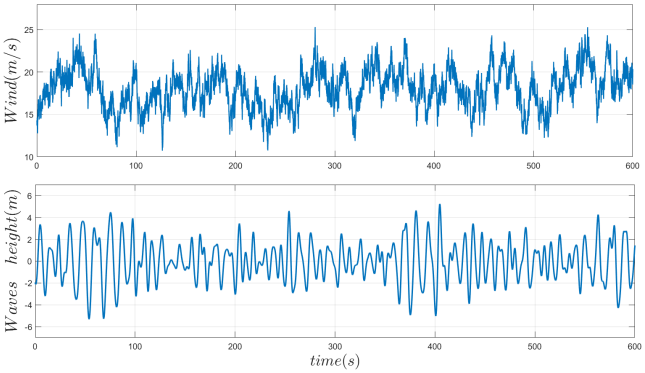

Fig. 3. Wind scenario (top) and wave height scenario (bottom)

The control parameters are listed as Table 1, where k_1 and k_2 are the controller gains of (19). The input of the RBFNN is $\mathbf{x} = [s\ \dot{s}]$. The number of neurons in the hidden layer of the network is $N = 5$, and the parameters of the Gaussian basis function are taken as $\mathbf{c} = [[-1\ -0.5\ 0\ 0.5\ 1]; [-1\ -0.5\ 0\ 0.5\ 1]]$, $b = 1$, $\eta_1 = 0.05$ and $\eta_2 = 0.5$.

B. Discussion

The simulation results comparing the performance of RBFNN-STSM-CBPC with STSM-CBPC and the baseline GSPI controller for FOWT are illustrated in Fig.4.

In Table II, the mean values and standard deviations (STD) for each signal are presented when the 50 first seconds of the simulation have been removed. Both the RBFNN-STSM-CBPC and STSM-CBPC controllers effectively regulate the rotor speed to its rated value. However, the proposed RBF-STSM-CBPC exhibits approximately half of the STD observed in both the STSM-CBPC and the Baseline. Moreover, the platform pitch angle θ_y and pitch rate ω_y are better regulated with lower STD compared to the RBFNN-STSM-CBPC and the Baseline. Therefore, in terms of control objectives, the RBFNN-STSM-CBPC outperforms the other two methods. It is noteworthy that SMC can introduce aggressive control inputs, evident in the wider variations of the blade pitch angle compared to the Baseline for both STSM-CBPC methods. There exists a trade-off that needs optimization between blade pitch angle variations and achieving control objectives, particularly in tracking the rotor's rated speed and minimizing platform pitch.

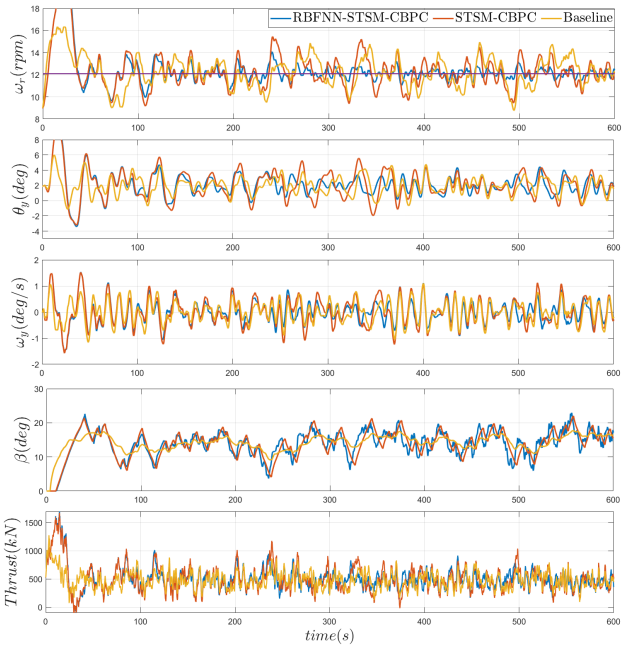

Fig. 4. Simulations results: RBF-STSM-CBPC, STSM-CBPC and baseline

TABLE II

MEAN ERRORS AND STANDARD DEVIATION RESULTS

Controllers	**Mean** ω_r [rpm]	**STD** ω_r [rpm]	**Mean** θ_y [deg]	**STD** θ_y [deg]
GSPI	12.0984	1.2258	1.9314	1.0776
STSM	12.1509	1.2064	2.0102	1.5294
RBF-STSM	12.1102	0.6538	2.0071	0.9674
	Mean ω_y [deg/s]	**STD** ω_y [deg/s]	**Mean** Thrust [kN]	**STD** Thrust [kN]
GSPI	0.0017	0.3919	472.7873	130.7851
STSM	-0.0035	0.4641	485.3420	178.9801
RBF-STSM	-0.0027	0.3493	486.8331	144.7849

V. CONCLUSION

This paper introduces the design of a RBFNN-STSM-CBPC for semi-submersible FOWTs. By incorporating the RBFNN to approximate lumped uncertainties and disturbances, the composite controller aims to regulate the rotor speed to its rated value while minimizing platform pitching motion. An error estimator compensates for the theoretical minimum estimation error of the neural network. The integration of these three components within the control scheme offers an adaptive control solution, leveraging the robustness of SMC and the estimation capabilities of neural networks. Simulation results validate the composite controller's effectiveness in addressing the complex dynamics and uncertainties inherent in FOWTs operating in Region III.

ACKNOWLEDGMENT

This work was supported by the ANR Project (CREATIF), the EIPHI Graduate School (contract ANR-17-EURE-0002) and the Region Bourgogne Franche-Comté.

REFERENCES

[1] T. Larsen and T. Hanson, "A method to avoid negative damped low frequent tower vibrations for a floating, pitch controlled wind turbine," *Journal of Physics: Conference Series*, vol. 75, p. 012073, Jul. 2007.

[2] J. Jonkman, "Dynamics modeling and loads analysis of an offshore floating wind turbine," National Renewable Energy Laboratory, Golden, Colorado, USA, Tech. Rep. NREL/TP-500-41958, Dec. 2007.

[3] G. Betti, M. Farina, G. Guargliardi, A. Marzorati, and R. Scattolini, "Development of a control-oriented model of floating wind turbines," *IEEE Trans. Control Syst. Technol*, vol. 22, pp. 69–82, Jan. 2014.

[4] F. Sandner, D. Schlipf, D. Matha, R. Seifried, and P. W. Cheng, "Reduced nonlinear model of a spar-mounted floating wind turbine," in *German Wind Energy Conference (DEWEK)*, Bremen, Germany, Nov. 2012.

[5] J. R. Homer and R. Nagamune, "Physics-based 3-d control-oriented modeling of floating wind turbines," *IEEE Trans. Control Syst. Technol*, vol. 26, no. 1, pp. 14–26, 2018.

[6] K. H. O. Baghernieh and R. Horowitz, "Nonlinear control of floating offshore wind turbines using input/output feedback linearization and sliding control," in *ASME Dynamic Systems and Control Conference*, San Antonio, Texas, USA, Oct. 2014.

[7] C. Zhang, E. Tahoumi, S. Gutierrez, F. Plestan, and J. Deleon-Morales, "Adaptive robust control of floating offshore wind turbine based on sliding mode," in *IEEE 58th Conference on Decision and Control*, Nice, France, Dec. 2019.

[8] F. P. C. Zhang, S. V Gutierrez and J. D. Leon-Morales, "Adaptive super-twisting control of floating wind turbines with collective blade pitch control," *IFAC-PapersOnLine*, vol. 52, pp. 6936–6941, Aug. 2019.

[9] J. M. Jonkman and M. L. Buhl, "Fast user's guide," in *Nat. Renewable Energy Lab.*, U.S. Dept. Energy, Golden, CO, USA, 2005.

[10] C. Zhang and F. Plestan, "Adaptive sliding mode control of floating offshore wind turbine equipped by permanent magnet synchronous generator," *Wind Energy*, vol. 24, pp. 754–769, Jan. 2021.

[11] M. Taleb, A. Marie, C. Zhang, M. A. Hamida, P.-E. Testelin, and F. Plestan, "Adaptive nonlinear control of floating wind turbines: new adaptation law and comparison," *IECON 2021 – 47th Annual Conference of the IEEE Industrial Electronics Society*, pp. 1–6, 2021.

[12] J. A. Moreno, "On strict lyapunov functions for some non-homogeneous super-twisting algorithms," *J. Frankl. Inst*, vol. 351, no. 4, pp. 1902–1919, 2014, special Issue on 2010-2012 Advances in Variable Structure Systems and Sliding Mode Algorithms.

[13] J. Fei and H. Ding, "Adaptive sliding mode control of dynamic system using rbf neural network," *Nonlinear Dyn*, vol. 70, no. 2, pp. 1563–1573, 2012.

[14] L. Wang, T. Chai, and L. Zhai, "Neural-network-based terminal sliding-mode control of robotic manipulators including actuator dynamics," *IEEE Trans. Ind. Electron.*, vol. 56, no. 9, pp. 3296–3304, 2009.

[15] Z. Feng and J. Fei, "Super-twisting sliding mode control for micro gyroscope based on rbf neural network," *IEEE Access*, vol. 6, pp. 64 993–65 001, 2018.

[16] A. Robertson, J. M. Jonkman, M. Masciola, A. G. H. Song, A. Coulling, and C. Luan, "Definition of the semisubmersible floating system for phase ii of oc4," National Renewable Energy Laboratory, Golden, Colorado, USA, Tech. Rep. NREL/TP-5000-60601, Sep. 2014.

[17] H. Basbas, Y.-C. Liu, S. Laghrouche, M. Hilairet, and F. Plestan, "Review on floating offshore wind turbine models for nonlinear control design," *Energies*, vol. 15, no. 15, 2022.

[18] Y.-C. Liu, H. Basbas, and S. Laghrouche, "Robust blade pitch control of semi-submersible floating offshore wind turbines based on the modified super-twisting sliding-mode algorithm," *Under Review*, 2024.

[19] W. M. J. M. Jonkman, S. Butterfield and G. Scott, "Definition of a 5-mw reference wind turbine for offshore system development," National Renewable Energy Laboratory, Golden, Colorado, Tech. Rep. NREL/TP-500-38060, Feb. 2009.

[20] F. Didier, Y.-C. Liu, S. Laghrouche, and D. Depernet, "A comprehensive review on advanced control methods for floating offshore wind turbine systems above the rated wind speed," *Energies*, vol. 17, no. 10, 2024.

[21] Y.-C. Liu, S. Laghrouche, A. N'Diaye, and M. Cirrincione, "Hermite neural network-based second-order sliding-mode control of synchronous reluctance motor drive systems," *J. Frankl. Inst*, vol. 358, no. 1, pp. 400–427, 2021.